Supplement of Weather Clim. Dynam., 4, 833–852, 2023
https://doi.org/10.5194/wcd-4-833-2023-supplement

Supplement of

Atmospheric bias teleconnections in boreal winter associated with systematic sea surface temperature errors in the tropical Indian Ocean

Yuan-Bing Zhao et al.

Correspondence to: Yuan-Bing Zhao (yuan-bing.zhao@uni-hamburg.de)

This supplement provides a brief description and discussion of the biases in the zonal-mean flow and the Walker circulation caused by the TIO SST biases.

The unbalanced zonal-mean flow is dominated by the meridional circulation (Pikovnik et al. 2022). Figure S1 shows its climatology and biases in the reference and sensitivity simulations, respectively. They are represented by the zonal-mean meridional mass stream-function (MSF) at 500 hPa (Yun et al. 2021). One can see that the Hadley cell (HC) in the Northern Hemisphere (in DJF) is the strongest component of the meridional circulation. It is confined between 10°S and 35°N. Visible biases in the meridional circulation are also confined in this region. In experiments with a positive TIO SST bias, the biases are opposite in phase to the reference HC, resulting in a weakening of the HC and the zonal-mean flow energy. In contrast, the biases align with the reference HC in the experiment with a negative SST bias, leading to a strengthening of the HC. Nevertheless, the overall bias amplitude is very small compared to the reference state and is likely not significant.

Regarding the balanced zonal-mean flow, the geopotential height increases in low-to-mid latitudes (45°S-45°N) due to the positive SST bias (EXP_NEG, EXP_10N, EXP_IOD) (Figs. S2a, S2c and S2d). The largest increase is observed in the subtropics, along with the strengthening of the westerlies in midlatitudes and easterlies in the tropics. The maximum change in the upper troposphere can reach 1.5 m s^{-1} (see Fig. S2d). Therefore, both kinetic and available potential energies increase. The opposite occurs in negative SST bias forcing (Fig. S2b). Note that the total energy in EXP_NEG increases, but the change is very small and is probably not significant (see Fig. 9b in the main text).

In the tropics, Walker circulation (WC) dominates the unbalanced wave fields. Figure S3a displays its climatology and biases in the reference and sensitivity simulations, respectively. They are represented by the tropical (10°S-10°N) mean zonal mass stream-function (MSF) at 500 hPa (Yun et al. 2021). The WC responses to TIO SST biases are generally strong. The WC bias is stronger in EXP_IOD than in other experiments. The WC and its biases are characterized by large scales (Fig. S3b). The reference WC is dominated by zonal wavenumbers 1-4. The WC biases in EXP_POS, EXP_NEG, and EXP_10N are all dominated by zonal wavenumbers 1-3, and that in EXP_IOD is dominated by the first 6 zonal wavenumbers. There are significant phase differences between the biases and the reference state (Fig. S3c). At zonal wavenumbers 1 and 2, the phase difference $\Delta\theta$ (see the caption of Fig. S3) between the biases in EXP_IOD and the reference state is approximately $3\pi/4$, while for the other experiments, the phase differences are slightly smaller than $\pi/2$. Therefore, EXP_IOD has a large negative bias covariance ($\propto A^R A^b \cos\Delta\theta$) at the first two zonal wavenumbers, which is responsible for the energy decrease (see Fig. 9c in the main text). In contrast, in the other experiments, the contribution of bias covariance to the energy changes is smaller compared to the contribution of bias variance ($\propto A^b A^b$) (see Fig. 9c in the main text).

All the figures below are based on PLASIM simulations.

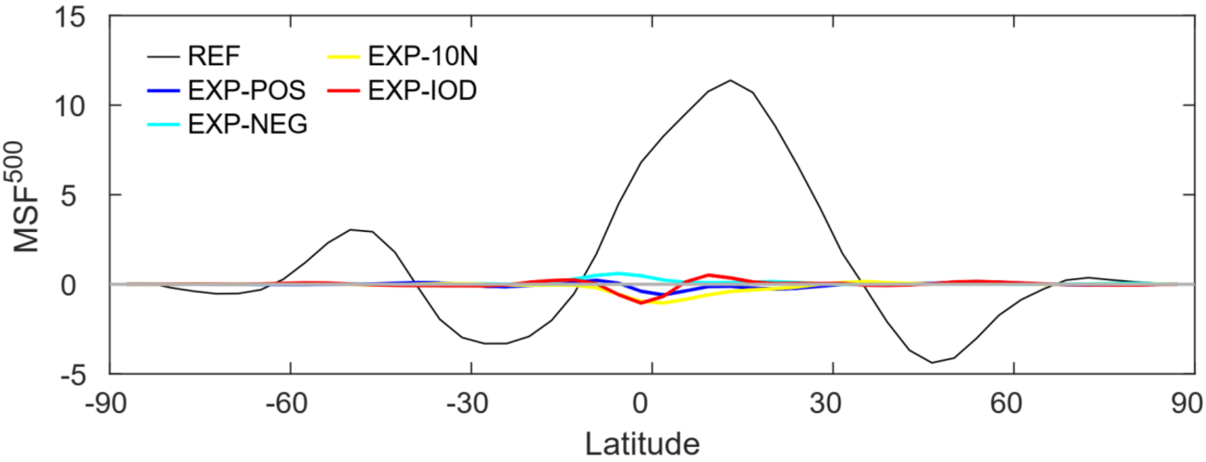

Figure S1. The climatology (black line) and biases (color lines) of the zonal-mean meridional mass stream-function (MSF; in 10^{10} Kg s^{-1}) at 500 hPa. The computation follows the method in Yun et al. (2021).

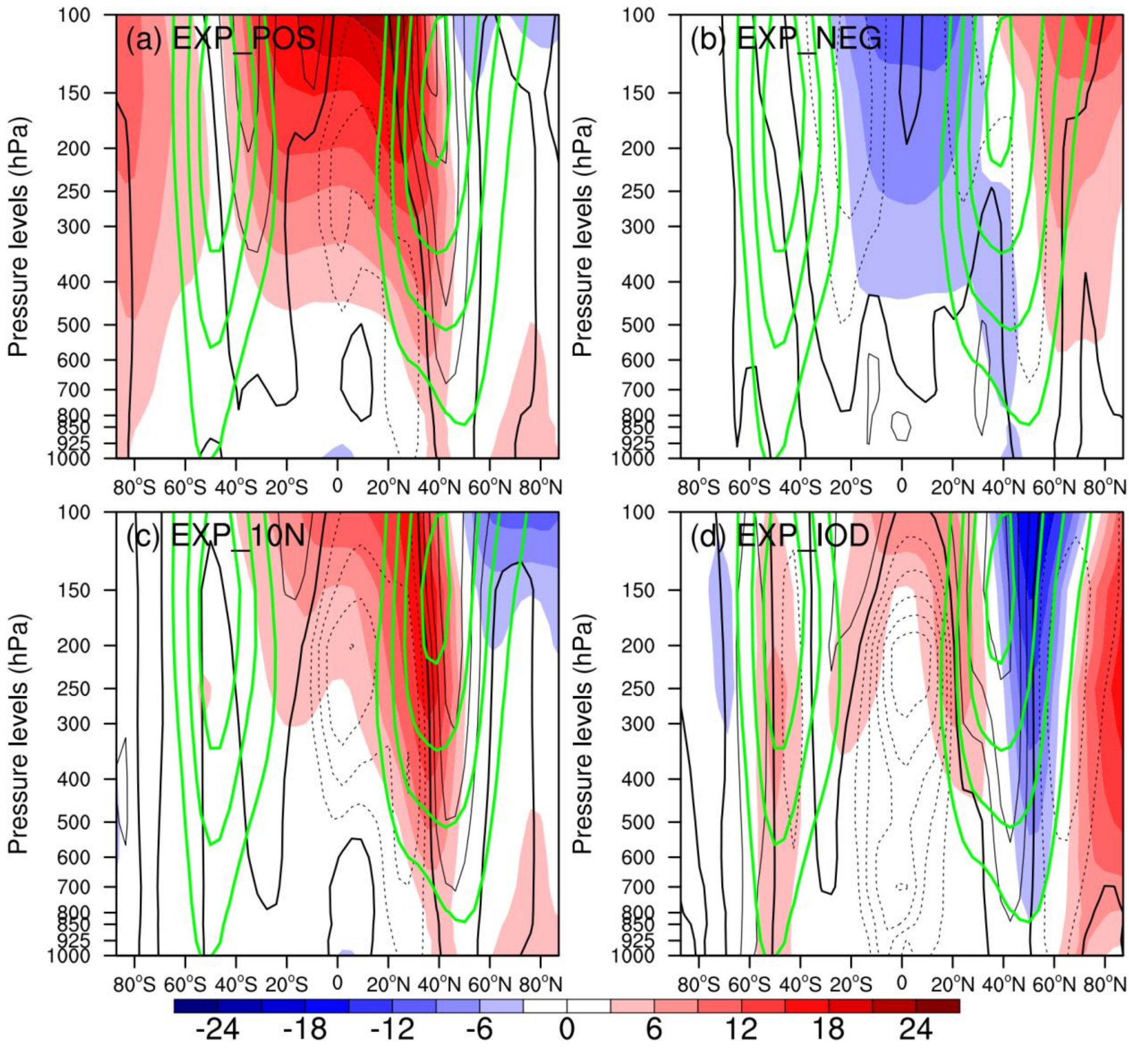

Figure S2. The zonal-mean biases of geopotential height (shadings; in gpm) and zonal wind (black contours; in m s^{-1}) in (a) EXP_POS, (b) EXP_NEG, (c) EXP_10N, and (d) EXP_IOD. Green contours show the background zonal wind (in m s^{-1}) with an interval of 10 m s^{-1}. Black contours are drawn at intervals of 0.3 m s^{-1}, with negative contours dashed and zero contours in bold.

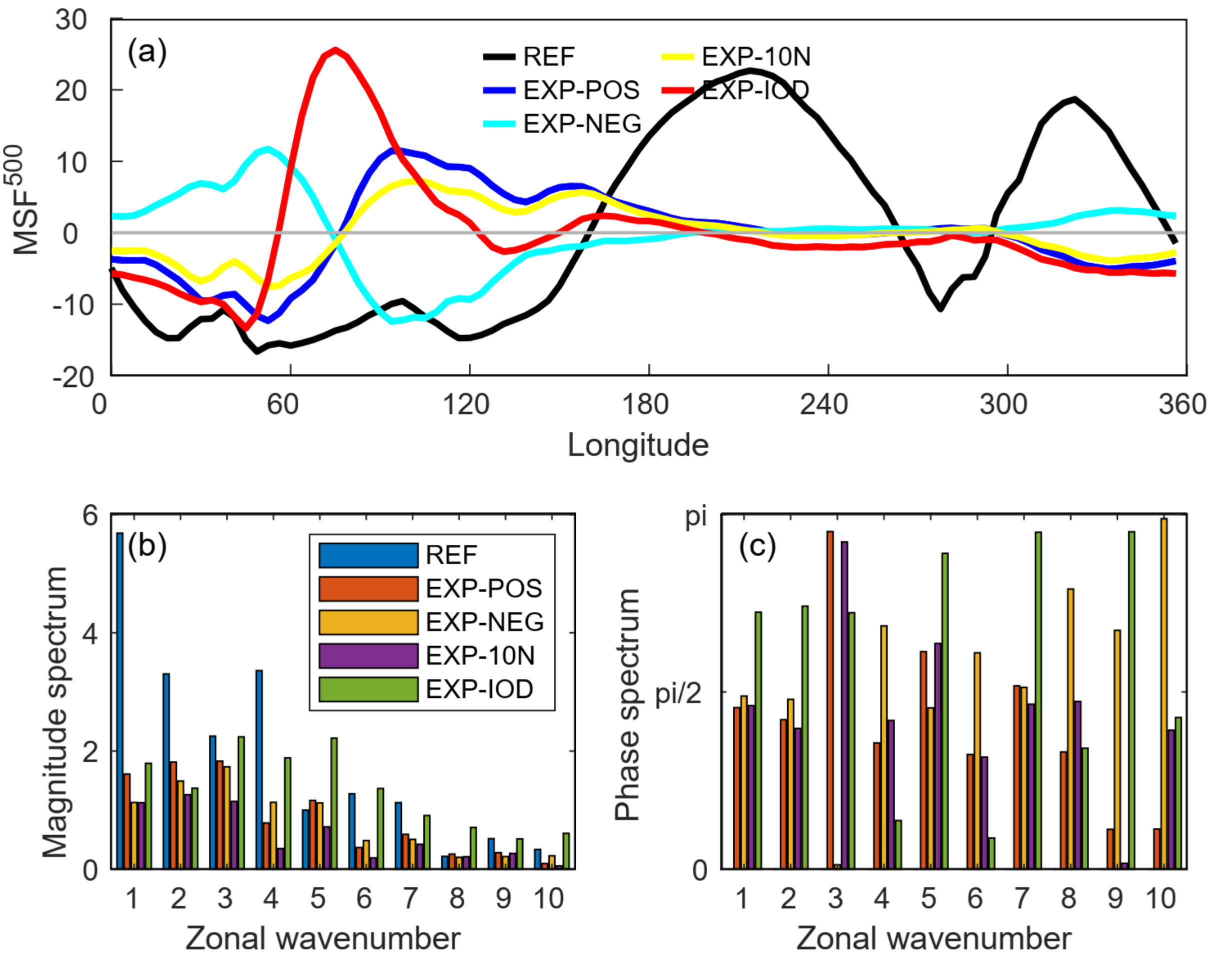

Figure S3. (a) The climatology (black line) and biases (color lines) of the tropical (10°S-10°N) mean zonal mass stream-function (MSF; in 10^{10} Kg s^{-1}) at 500 hPa which represents the Walker circulation. The computation follows the method in Yun et al. (2021). Let the climatology be $\mathrm{MSF}^{500}_{\mathrm{ref}} = A^{\mathrm{R}}\mathrm{e}^{i\theta^{\mathrm{R}}}$ and the bias in sensitivity experiments be $\mathrm{MSF}^{500}_{\mathrm{bias}} = A^{\mathrm{b}}e^{i\theta^{\mathrm{b}}}$, (b) and (c) show, respectively, the spectra of the amplitude (A^{R} and A^{b}) and the absolute phase difference between the bias and the climatology ($\Delta\theta = |\theta^{\mathrm{b}} - \theta^{\mathrm{R}}|$).

References:

Pikovnik, M., Ž. Zaplotnik, L. Boljka, and N. Žagar, 2022: Metrics of the Hadley circulation strength and associated circulation trends. *Weather and Climate Dynamics*, **3**, 625–644, https://doi.org/10.5194/wcd-3-625-2022.

Yun, K.-S., A. Timmermann, and M. F. Stuecker, 2021: Synchronized spatial shifts of Hadley and Walker circulations. *Earth System Dynamics*, **12**, 121–132, https://doi.org/10.5194/esd-12-121-2021.